The 2009 IEEE/RSJ International Conference on
Intelligent Robots and Systems
October 11-15, 2009 St. Louis, USA

Analysis and Optimal Design of a Modular Underactuated Mechanism for Robot Fingers

Shuangji Yao, Licheng Wu, Marco Ceccarelli, Giuseppe Carbone and Zhen Lu

***Abstract*—A frame of modular design problems and requirements for underactuated mechanisms is discussed as related to robotic fingers. The proposed modular mechanism is connected sequentially by series units of underactuated mechanisms, which have the feature of passive self-adaptive in grasp operation and uniformizable in design procedure. The design considerations for modular underactuated mechanism are outlined. Optimality criteria are analyzed with the aim to formulate a general design algorithm. An example of a four-phalanx modular robotic finger is studied as an improvement of new version LARM Hand with the aim to show the practical feasibility for the proposed modular concepts and design methods.**

I. Introduction

The aim of underactuated mechanisms is to reduce the number of degrees of freedom and actuators with low-cost easy-operation features for applications in robotics and other fields. Several solutions are proposed as robotic hands in the literature with tendon or linkage structures, as in [1-5]. Linkage-based mechanisms are usually preferred for applications where large grasping forces are requested. They can performance enveloping motion to grasp large objects stably as desired. The feature of enveloping grasp are studied by many researchers. An analysis is reported in [6] for an enveloping grasp using frictionless contact. A design procedure for a two-phalanx underactuated finger is presented in [7] with grasp stability issues. A novel multi-finger underactuated mechanism is proposed in [8] with torsion springs in the joints. A robotic hand with two fingers with 3 phalanxes is reported in [9]; each of the fingers is actuated by 4 pneumatic cylinders for underactuated mechanisms. In [10] the authors proposed a design of a finger that is based on underactuated linkage mechanism and coupling linkage. A design of compact bio-mimetic fingers with compliant mechanisms is reported in [11] as embedded in the finger body during the grasping operation.

Manuscript received February 28, 2009. Part of this work has been developed within the project No.27 of the Italy-China program 2006-2009 and has been supported by Key International S&T Cooperation Project with grant number 2008DFA81280. This work is also supported by the NSFC Project 60875062 and Innovation Foundation of BUAA for PhD Graduates.

Shuangji Yao and Zhen Lu are with the School of Automation Science and Electrical Engineering, Beihang University, Beijing P.R.China (e-mail: buaayaoshuangji@ 163.com).

Licheng Wu is with the College of Information Engineering, Central University for Nationalities, Beijing, P.R.China (e-mail: wulichenggg @hotmail.com).

Marco Ceccarelli and Giuseppe Carbone are with LARM: Laboratory of Robotics and Mechatronics, University of Cassino, Cassino (Fr), Italy (e-mail: ceccarelli@unicas.it).

Since the early 1990s at LARM, a research line has been devoted for designing low-cost easy-operation grasping anthropomorphic fingers as reported in [12]. Solutions with underactuated mechanisms and flexible mechanisms have been carefully discussed in [13], in order to improve the capability of grasping objects with different sizes and shapes.

It is useful to develop a modular finger mechanism which is based on underactuated linkage mechanisms. This kind of mechanisms has of low-cost easy operation features, and they can perform enveloping grasp for most of the grasping tasks. Modular mechanisms have suitable characteristics for an iterative design procedure. For general requirements, design considerations have been summarized and formulated for modular underactuated finger mechanisms in this paper as criteria in a optimization design procedure.

II. Modular Design for Underactuated Finger Mechanisms

Passive elements can be used to constrain the kinematics of a finger, such as torsion springs and linear springs. For example, a new type of underactuated finger is proposed in [14] and is based on linkage mechanism with passive elements as studied at LARM. Feasible design schemes are shown in Fig. 1. Those kinematic designs for a new underactuated finger are based on four-bar mechanisms with torsion springs and linear springs in different phalanxes. They can perform self-adaptation to grasp objects with different shape and size within a certain range. Moreover, such underactuated mechanism can remain fully embedded in the finger body. Nevertheless, this result can be only obtained through a careful dimensional synthesis of the mechanism. This dimensional synthesis can be also achieved via a multi-objective optimization problem.

A modular mechanism can be considered as a mechanism whose design is obtained by repetition of sub-systems whose output is the input for the next one in the kinematic chain. In addition, each module can have a full functionality that nevertheless characterizes the operation of the overall design.

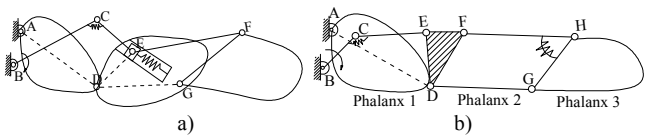

Fig. 1 Kinematic design schemes for new linkage underactuated finger mechanisms.

In this paper, a specific attention has been addressed in choosing as modules underactuated mechanisms with linkage

design and spring elements. Advantages in using modular mechanism for finger design can be identified in aspects that enhance the easiness of the operation, the compactness and maintenance of the design, and unified standards of the mechanical design. In addition, underactuation in robotic hand grasping gives fewer actuators than degrees of freedom, as reported in [15]. This gives the character of simple control adapting to objects shape automatically as an advantage of the mechanical intelligence for the design of robotic fingers.

III. Design Considerations

In order to satisfy general design requirements, design considerations should be summarized and formulated as criteria in a design procedure. Considerations include the efficiency, force, anthropomorphic, tolerances, size, capability, compactness. Thus, a design for a robot finger must fulfill basic features, such as motion transmission, actuation efficiency, underactuation operation, position error and tolerances analysis, grasping capability, compact mechanical design, light-weight design.

A. Motion Transmission

A proper motion transmission in underactuated modular mechanisms is due to the transmission angles between consecutive units since they are also the rotation angles of the phalanxes. The angle between the coupler link and follower link in a four-bar mechanism is called as the transmission angle. The input torque is affected by transmission angles to actuate a phalanx. As a transmission angle becomes small, the mechanical transmission can be extremely difficult, so that even a small amount of friction will cause the mechanism to lock or jam as pointed in any handbook. A common rule from engineering practice is that a four-bar linkage should not be used in the region where the transmission angle is less than 40 deg or larger than 130 deg.

Referring to the scheme in Fig. 2 for a N-modular finger mechanism, when phalanx 1 contacts an object, the point of B on the link P_2 will not move any more, and the angle of S_1 will begin to change. Thus, the next unit phalanx 2 will be actuated through link AA_1 and link A_1B^*. When a finger body of phalanx i contacts an object, it will be stop on the object surface. An equivalent mechanism of phalanx (i+1) contacting an object can be modeled as in Fig. 3, in which link IJ stops against the surfaces of the object after phalanx i contacts an object. Joint I and J will not move any more, but link P_i continues rotating to actuate the next linkage mechanism unit.

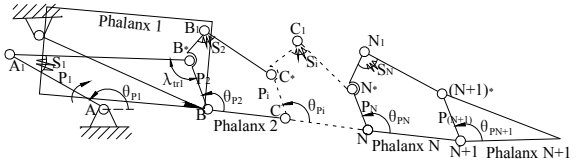

Fig. 2 A modular underactuated finger mechanism with 1 active DOF.

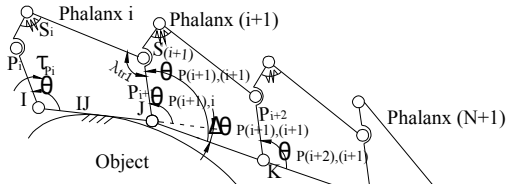

Fig. 3 An equivalent mechanism for modular robotic finger mechanism when (i+1)-th phalanx contacts an object.

At the same time the torsion spring S_i in phalanx i begins to extend, link P_{i+1} begins to rotate around the joint J and the other phalanxes continue to envelope the object. When the next phalanx contacts the object, link JK stops against the object surface. As shown in Fig. 3, $\theta_{P(i+1),i}$ refers to the rotation angle of link $P_{(i+1)}$ when i-th phalanx stops on the object surface, and $\Delta\theta_{P(i+1),(i+1)}$ refers to the additional rotation angle of the (i+1)-th phalanx after i-th phalanx contacts the object. Thus, after phalanx i contacts an object, the angle parameter $\theta_{Pi,I}$ can be computed as $\theta_{P,i} = \theta_{P,(i+1)}$, in which $\theta_{Pi,m}$ is the angle of link P_i after that m-th phalanx contacts the object. The rotation angle $\theta_{P(i+1),(i+1)}$ can be given as

$$\theta_{P(i+1),(i+1)}=\theta_{P(i+1),i}+\Delta\theta_{P(i+1),(i+1)} \tag{1}$$

where $\Delta\theta_{P(i+1),m}$ indicates the additional rotation angle of link $P_{(i+1)}$ after i-th link contacts the object. Then, when phalanx (i+1) contacts the object, the angle of link P_{i+2} can be computed equal from the previous module in Fig. 3. Therefore if phalanx 2 contacts the object the point C will not move any more, the angle of link P_3 can be given as, Fig. 2,

$$\theta_{P3,2}=\theta_{P3,1}+\Delta\theta_{P3,2} \tag{2}$$

Therefore the angles of other links $P_{i,2}$ will remain equal to $\theta_{P3,2}$. Thus, if there are N+1 phalanxes in the modular finger mechanism, after the N-th phalanx contacts the object the angle of link $P_{(N+1)}$-th can be expressed as

$$\theta_{P(N+1),N}=\theta_{P(N+1),(N-1)}+\Delta\theta_{P(N+1),N} \tag{3}$$

Consequently, when the final phalanx contacts the object the angle of link $P_{(N+1)}$ can be computed as

$$\theta_{P(N+1),(N+1)}=\Delta\theta_{P(N+1),(N+1)}+\Delta\theta_{P(N+1),N}+\cdots+\Delta\theta_{P2,1}+\theta_{P2,0} \tag{4}$$

In order to compute the transmission angle for each phalanx, a single phalanx module can be analyzed as in Fig. 3, where θ_{Pi} is the input angle for the i-th four-bar linkage module and θ_{Pi+1} is its output angle. If the dimension of the four-bar linkage is given, a function for the input-output angles can be formulated as $\theta_{Pi+1} = f(\theta_{Pi})$. Another function can also be defined as $f_\lambda(\theta_{Pi+1})= \lambda_{tri}$ to express the relationship between the transmission angles λ_{tri} and the input angle θ_{Pi+1}. The angles λ_{tri} and θ_{Pi} are given by the dimension parameters of the linkage mechanism. In Fig. 2 for example, the transmission angle is given by $\lambda_{tr1}=A_1B^*B$, and the

relationship between transmission angle λ_{tr1} and the θ_{P2} can be expressed as $\lambda_{tr1} = f_\lambda(\theta_{P2})$. A modular four-bar mechanism can be designed to achieve a performance with $\theta_{Pi+1}/\theta_{Pi} > 1$, so that θ_{P1} is the smallest among all θ_{Pi}. The transmission angle range of the first phalanx is the largest than others. Thus, the restriction on λ_{tr1} can be expressed as the smallest transmission angle for the whole finger mechanism.

In general grasping tasks, the finger envelopes objects in a motion plane when they have a regular surface like cylinders. At the final configuration, each phalanx link can be considered as a segment of a polygon enveloping the object boundary. Thus, the additional angle for each phalanx motion $\Delta\theta_{P(i+1),i}$ equals to $\Delta\theta_P$. The angles for the (N+1)-th phalanx can be expressed from (3) and (4) as

$$\theta_{P(N+1),(N+1)} = f_{(i+1),i}(\cdots f_{2,1}(\theta_{P1}+\Delta\theta_P)\cdots)+\Delta\theta_P \quad (5)$$

The restriction for transmission angle can be expressed as

$$\lambda_{tr,1} = f_\lambda(\theta_{P2}) \geq 40^\circ; \lambda_{tr,N} = f_\lambda(\theta_{P(N+1),(N+1)}) \leq 130^\circ \quad (6)$$

B. Actuation Efficiency

The maximum input torque τ_{in} can be optimized in a design process for an efficient grasping process, with the aim to have the smallest actuator as possible.

A suitable contact model of the modular finger mechanism can be proposed as Fig. 4 at a final grasping configuration, where f_i: contact force for each phalanx; $\mathbf{r}_i$: vector for each link in the mechanism; W: the weight of grasped object; R: the radius of grasped segment cylindrical object; τ_{in}: input torque for the actuator; S_i: torsion spring efficient; θ_{Pi}: the phalanx angle; β_i: the angle of the phalanx force. According to the Principle of Virtual Work, the relationship between external forces on each phalanx and corresponding driving force for finger mechanism can be written as

$$\boldsymbol{\tau} = \mathbf{J}^T\mathbf{f}_e \quad (7)$$

where $\mathbf{f}_e$: the vector of external forces acting on the phalanxes; $\boldsymbol{\tau}$: the vector of input torques of the modular finger mechanism system; $\mathbf{J}$: the Jacobian matrix of the proposed mechanism which can be formulated by using kinematics relationship.

The friction at the contact surface can be neglected at the design stage since this condition is conservative both for static equilibrium of a grasp and for grasp tasks with low-friction objects. Thus, the contact torque in vector of external forces $\mathbf{f}_e$ can be zero and vector $\mathbf{f}_e$ can be given as

$$\mathbf{f}_e = [0,\cdots 0, f_1\cos\beta_1, f_1\sin\beta_1,\cdots,f_{N+1}\cos\beta_{N+1}, f_{N+1}\sin\beta_{N+1}]^T \quad (8)$$

$$\boldsymbol{\tau} = [\tau_{in}\ \tau_{S1}\cdots\tau_{S(N+1)}]^T \quad (9)$$

$$\mathbf{J} = \frac{\partial[\theta_{P1},\cdots,\theta_{PN}, x_1, y_1,\cdots,x_{N+1}, y_{N+1}]^T}{\partial[\theta_{in}, \theta_{S1},\cdots,\theta_{S(N+1)}]^T} \quad (10)$$

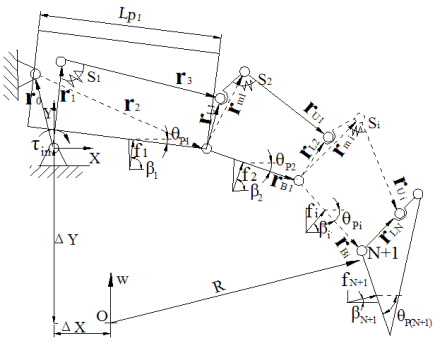

Fig. 4 A contact model for modular underactuated finger mechanism.

where τ_{Si}: the torque of each torsion spring; X_i, Y_i: the positions of the contact force location in XY frame in Fig. 4.

By using (8), (9) into (7), the relationship among contact force and driving torque and spring torque can be given as

$$[\tau_{in}, \tau_{S1},\cdots,\tau_{S(N+1)}]^T = \mathbf{J}^T[0,\cdots,0, f_1c\beta_1, f_1s\beta_1,\cdots, f_{N+1}c\beta_{N+1}, f_{N+1}s\beta_{N+1}]^T \quad (11)$$

Therefore, the equilibrium can be formulated in the form $\boldsymbol{\tau} = \mathbf{U}\mathbf{f}_i$, where $\mathbf{f}_i$ is the vector of contact forces $[f_1,\ldots,f_{N+1}]^T$, $\mathbf{U}$ is a matrix containing Jacobian matrix.

Considering the actuator torque for grasping efficiency, an optimality criterion can be expressed as to minimize the actuator torque, with restrictive conditions as $f_i > 0$.

C. Underactuated Operation with Spring System Design

Design considerations includes aspects for the spring design, since energy can be stored in the springs. The spring coefficients k_i can be computed from (11) as

$$\begin{bmatrix} \tau_{in} \\ k_1 \\ \vdots \\ k_{(N+1)} \end{bmatrix} = \begin{bmatrix} 1 & & & \\ & 1/(\Delta\theta_{S1}) & & \\ & & \ddots & \\ & & & 1/(\Delta\theta_{S(N+1)}) \end{bmatrix} \mathbf{U}\mathbf{f}_i = \mathbf{V}\mathbf{f}_i \quad (12)$$

in which $\Delta\theta_{Si}$ is the difference of i-th spring angles between final configuration and initial configuration. The matrix $\mathbf{V}$ contains angle parameters and matrix $\mathbf{U}$. Thus, the coefficient for each torsion spring k_j can be computed as

$$k_j = \sum_{i=1}^{N+1} \mathbf{V}_{i+1} f_i \quad (13)$$

where $\mathbf{V}_{i+1}$ is the (i+1)-th column of matrix $\mathbf{V}$. The energy which is stored in the torsion spring system at a final configuration, can be formulated as

$$E = \frac{1}{2}\sum_{i=1}^{N+1} k_i(\theta_{Si} - \theta_{Si,0})^2 \quad (14)$$

Thus, an optimality criterion for the spring system design can be expressed as to minimize the stored energy E in (14).

D. Position Error and Tolerances Analysis

A modular mechanism may accumulate a large amount of position errors in a series of modules. As for example in Fig. 4, the position error of joint (N+1) in the final module is affected and accumulated from previous mechanism modules. A mechanical position error can be represented as a deviation from a prescribed point position as reported in [16]. The prescribed position can be computed by using the design values for all mechanism modules as the input parameters. A direct linearization function approaches is provided and an application to position error in kinematic linkages is introduced in [17]. This approach can be applied also to the design of modular finger mechanisms.

In Fig. 4, for a given input link $\mathbf{r}_1$, the position of point (N+1) in the final module $\mathbf{P}_{(N+1)}$ can be computed by solving closed loops and one open loop for the over all finger mechanism. Referring to Fig. 4, the closed loops can be expressed as

$$\mathbf{r}_0 + \mathbf{r}_2 - \mathbf{r}_1 - \mathbf{r}_3 - \mathbf{r}_{L2} = \mathbf{0} \tag{15}$$

$$\mathbf{r}_{mi} + \mathbf{r}_{Ui} - \mathbf{r}_{Bi} - \mathbf{r}_{Li} = \mathbf{0} \quad (i=2,\ldots,N) \tag{16}$$

These equations can be expanded into 2N equations by using components in X and Y directions, in the form

$$\begin{aligned} h_1(\,) &= r_0\cos\theta_{r_0} + r_2\cos\theta_{r_2} - r_1\cos\theta_{r_1} - r_3\cos\theta_{r_3} - r_{L1}\cos\theta_{r_{L1}} \\ h_2(\,) &= r_0\sin\theta_{r_0} + r_2\sin\theta_{r_2} - r_1\sin\theta_{r_1} - r_3\sin\theta_{r_3} - r_{L1}\sin\theta_{r_{L1}} \\ &\vdots \\ h_{2N-1}(\,) &= r_{mN}\cos\theta_{r_{mN}} + r_{UN}\cos\theta_{r_{UN}} - r_{BN}\cos\theta_{r_{BN}} - r_{LN}\cos\theta_{r_{LN}} \\ h_{2N}(\,) &= r_{mN}\sin\theta_{r_{mN}} + r_{UN}\sin\theta_{r_{UN}} - r_{BN}\sin\theta_{r_{BN}} - r_{LN}\sin\theta_{r_{LN}} \end{aligned} \tag{17}$$

where all the angles Fig. 4 are measured from the positive X axis to its vector in counterclockwise direction. The design position $\mathbf{P}_{(N+1)}$ can also be computed by using open loop equations for the finger mechanism chain in term of X and Y components in the form

$$X_{(N+1)} = r_0\cos\theta_{r_0} + r_2\cos\theta_{r_2} + r_{B1}\cos\theta_{r_{B1}} + L + r_{BN}\cos\theta_{r_{BN}} \tag{18}$$

$$Y_{(N+1)} = r_0\sin\theta_{r_0} + r_2\sin\theta_{r_2} + r_{B1}\sin\theta_{r_{B1}} + L + r_{BN}\sin\theta_{r_{BN}} \tag{19}$$

The equations of closed loop can be linearized by using first-order Taylor's series expansion to give

$$[\mathbf{A}][\Delta\mathbf{X}] + [\mathbf{B}][\Delta\mathbf{U}] = [\mathbf{0}] \tag{20}$$

where [**X**] is the vector of independent variables, [**X**]=[r_2, r_3, r_{Li}, r_{ui}, r_{mi}, r_{Bi}]; [**U**] is the vector of dependent variables, [**U**]=[θr_2, θr_3, θr_{Li}, θr_{ui}, θr_{mi}, θr_{Bi}]; [**A**] and [**B**] are matrices of first-order partial derivatives with respect to the independent and dependent variables, and they can be computed by

$$[\mathbf{A}] = (\partial h_i)/(\partial \mathbf{X}_j) \tag{21}$$

$$[\mathbf{B}] = (\partial h_i)/(\partial \mathbf{U}_j) \tag{22}$$

Matrix [Δ**U**] can be computed from (20) in the form

$$[\Delta\mathbf{U}] = -[\mathbf{B}]^{-1}[\mathbf{A}][\Delta\mathbf{X}] \tag{23}$$

The same procedure can be applied to the system of the open vector loop, and the linearized equation can be expressed as

$$[\mathbf{C}][\Delta\mathbf{X}] + [\mathbf{D}][\Delta\mathbf{U}] = [\Delta\mathbf{P}_{(N+1)}] \tag{24}$$

where matrices [**C**] and [**D**] are computed by

$$[\mathbf{C}] = (\partial(\mathbf{N}+\mathbf{1}))/(\partial\mathbf{X}_j) \tag{25}$$

$$[\mathbf{D}] = (\partial(\mathbf{N}+\mathbf{1}))/(\partial\mathbf{U}_j) \tag{26}$$

where $\mathbf{P}_{(N+1)}$ is a vector [$X_{(N+1)}$, $Y_{(N+1)}$] in (18) and (19).

Therefore, a sensitivity matrix [**S**] for the position error analysis can be solved by substituting (23) into (24) to obtain

$$\Delta\mathbf{D}_{(N+1)} = ([\mathbf{C}] - [\mathbf{D}][\mathbf{B}]^{-1}[\mathbf{A}])(\Delta\mathbf{X}) = [\mathbf{S}][\Delta\mathbf{X}] \tag{27}$$

in which [$\mathbf{C}$-$\mathbf{DB}^{-1}\mathbf{A}$] is the sensitivity matrix **S** which represents changes in the independent variables as affected by the position errors. Thus, the worst-case position error can be expressed as

$$\Delta\mathbf{D}_{(N+1)} = \sum_{j=1}^{n} \left|\mathbf{S}_{ij}\right| \mathrm{tol}_j \tag{28}$$

where tol_j is the worst tolerance that is associated with the j-th independent variable. Thus, the function of F-norm ||**S**|| for sensitivity matrix **S** can be used as an optimal criterion of position errors in a design procedure.

E. Grasping Capability and Compact Mechanical Design

Grasping capability refers to the size and weight of objects that can be grasped. The maximum dimension that a modular mechanism can reach should be considered both as accessible working space and final grasping configuration. In Fig. 4, final grasping configuration of a finger mechanism can be identified when it envelopes cylindrical objects. The static equilibrium for phalanx contact forces can be expressed in the plane of the grasp. Therefore, the maximum radius *R* of the largest grasped object can be computed as

$$R = L_{p1}\cos\theta_{P1} + \sum_{i=2}^{N+1} r_{Bi}\cos\theta_{Pi} - r_0\cos\theta_{r_0} - \Delta X \tag{29}$$

The dimension along Y axis for the final grasping configuration can be computed as

$$\Delta Y = r_2\sin\theta_{r_2} + \sum_{i=2}^{N+1} r_{Bi}\sin\theta_{Pi} - r_0\sin\theta_{r_0} \tag{30}$$

Regarding the maximum weight, it can be computed from the static equilibrium for the contact forces balancing the object weight. Referring to Fig. 4, neglecting the friction

forces, the equilibrium of contact forces and gravity force of object W along Y direction can be expressed as

$$W_{max} = \sum f_i \sin\beta_i \tag{31}$$

Substitute $\boldsymbol{\tau}=\mathbf{U}\mathbf{f}_i$ into (31) it yields

$$W_{max} = \sum \mathbf{U}_i^{-1}\tau \sin\beta_i \tag{32}$$

in which $\mathbf{U}^{-1}{}_i$ is the i-th row of the matrix $\mathbf{U}^{-1}$.

The maximum grasping dimension can also be combined with the concept of compact design, by using a ratio between maximum grasping size and the total dimension of a modular finger mechanism. The dimension of a modular finger mechanism can be computed as the sum of the phalanx links. Therefore, an optimal criterion for both maximum grasping size and compactness structure can be expressed in the form

$$\text{ratio}_C = R_{max} \Big/ \sum_{i=1}^{N} L_i \tag{33}$$

IV. General formulation for Optimum Design

A design process with multiple design aspects should take into account simultaneously several design criteria. Since each of them can provide contradictory results, the design process can be conveniently conceived as multi-objective optimization problem in order to consider all the design criteria at same time. Thus, an optimum design for modular underactuated mechanisms can be formulated conveniently as

$$\min[\mathbf{F}(\mathbf{X})] = \min\{\max_{i=1,\ldots N}[w_i f_i(x)]\} \tag{34}$$

Subject to $\mathbf{G}(\mathbf{X}) < 0$ (35)

where min is the operator for calculating the minimum of a vector function $\mathbf{F}(\mathbf{X})$; max determines the maximum value among the N weighted functions $w_i f_i(x)]$ at each iteration; $\mathbf{G}(\mathbf{X})$ is the vector of constraint functions for restrictive limiting conditions. $\mathbf{X}$ is the vector of design variables; w_i is a weighting factor for the i-th objective function.

The design problems can be numerically solved by using a numerical procedure in commercial software package of MATLAB [18]. Multi-objective optimization is concerned with the minimization of multiple objective functions. The first step in an optimization process consists of selecting proper design variables, which are the geometrical parameters such as link lengths and angles. The variables are included in the vector $\mathbf{X}$ of (34). A suitable initial guess solution for the design parameters must be prescribed in the computational procedure. It will improve the execution efficiency and can help locate the global minimum instead of a local minimum. What should also be considered are the weighting factors, as from engineering viewpoint. For this paper, the MATLAB toolbox minimax algorithm has been used as numerical technique to solve the formulated optimization problem. Solutions that are generated in each iteration will consider the linear and nonlinear restrictive conditions in (35).

V. An example for a modular four-phalanx finger design in LARM Hand

A case of study has been investigated for an underactuated modular mechanism design that could be applied to the LARM Hand. The design scheme in Fig. 5 which is derived from Fig. 2 has been chosen as an example. In Fig. 5, unit one is a cross five-bar linkage and the modular mechanisms are from unit two to unit four, with linkage dimensions (r_{Li}, r_{Bi}, r_{ui}, r_{mi}). The mechanism has only one active DOF and three passive DOFs with torsion springs. Link r_0 of 16 mm is the base link and angle θ_{r0} is of 112 deg. Links r_2, r_{B1}, r_{B2}, r_{B3}, are contacting surfaces for the finger mechanism. A torsion spring S_1 is fixed on link r_1 and r_3 as installed parallel to the rotation joint B. The other two torsion springs S_2 and S_3 are fixed in the second and third phalanx joint C and G, respectively. The motor is installed at the joint A and it drives directly link r_1.

The optimality criteria in (34) can be used as objective functions for normalized computations in the design problems with weight coefficients w_i (i=1, 2, 3, 4, 5) as

$$\text{Min}\{\text{Max}[\mathbf{F}(\mathbf{X})]\} = \text{Min}\{\text{Max}[w_i f_i(x)]\} \tag{36}$$

when the objective function are given by

$$\begin{aligned} &f_1(x) = \tau/\tau_0\ ;\ \ f_2(x)=E/E_0\ ;\ \ f_3(x)=\|S\| \,/\, \|S\|_0 \\ &f_4(x) = \text{ratio}_C / \text{ratio}_{C,0};\ \ f_5(x) = W_{max} \end{aligned} \tag{37}$$

$$\begin{aligned} \text{Subject to}\ \ & g_1 = r_i>0;\ \ g_2 = 0< \alpha_1 <45^o;\ \ g_3 = 0< \alpha_2 <90^o \\ & g_4 = 0< \theta_{r1} <180^o;\ \ g_5 = 0< \theta_{Si} <180^o \\ & g_6 = 5N< f_i < 15N;\ \ \ g_7 = 40^o < \lambda_{tri} <130^o \end{aligned} \tag{38}$$

In particular, $f_1(x)$ in (37) represents the optimal criterion for actuator torque in link r_1. The expression $f_2(x)$ in (37) represents the energy ratio for the spring systems as deduced from (14). $f_3(x)$ describes the optimal criterion for the F-norm $\|\mathbf{S}\|$ of sensitivity matrix $\mathbf{S}$ in (28). $f_4(x)$ is the ratio for compactness in (33). Finally, $f_5(x)$ represents the ratio of maximum weight for the grasping capability in (32). Equations (38) represent design constraints. Particularly, the first constraint equation g_1 is positive definite in order to ensure link parameters of the driving mechanism with positive definite practical values. The second to fifth equations are geometric constraints for the link parameters. The sixth constraint equation g_6 represents the contact forces for each unit in a reasonable value between 5N and 15N. The equation g_7 is the restrictive condition for the transmission angles at the final configuration as expressed in (5) and (6).

Fig. 6 shows numerical evolution for the computed objective functions and design parameters as converging to optimal minimum values after 838 iterations with a CPU time of 317sec in an Itel Centrino Duo PC. The evolution and final solutions are shown in Fig. 7 and Table 1. Fig. 6 b) shows the

evolution for the link sizes. Design parameters and design constraints for the optimal solution are listed in Tables 2. The spring coefficients can be computed from (13) as k_1=0.045 Nm/rad, k_2=0.097 Nm/rad, k_3=0.177 Nm/rad. The constraint of transmission angles at the final configuration are computed from (5) and (6) as λ_{tr1}=48.7 deg, λ_{trN}=121.4 deg.

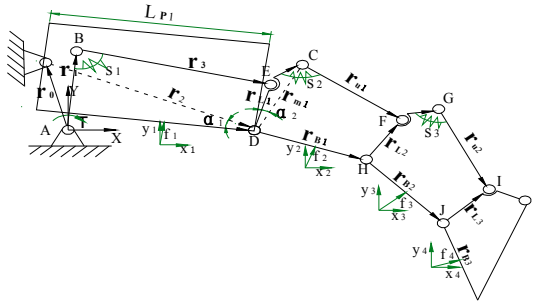

Fig. 5 A case for study with a four phalanxes underactuated robotic finger.

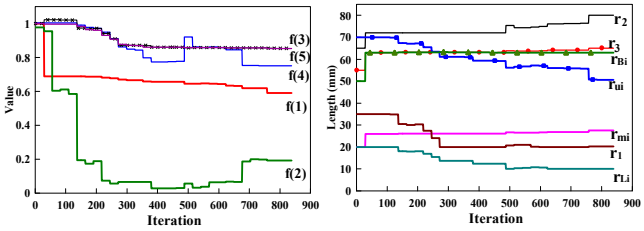

Fig. 6 Evolution of objective functions and design parameters for the numerical example: a) objective functions; b) design parameters.

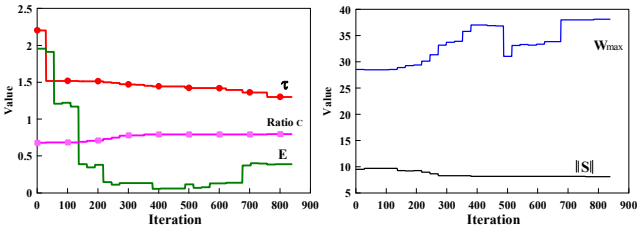

Fig. 7 Evolution of design items for the numerical example.

TABLE 1. INITIAL DATA AND OPTIMUM SOLUTION OF DESIGN CRITERIA

	τ (Nm)	E (Nm)	‖S‖	ratio C	W_{max} (N)
Initial data	2.200	1.955	9.506	0.680	28.534
Optimum solution	1.299	0.387	8.119	0. 796	31.406

TABLE 2. DESIGN PARAMETERS FOR THE OPTIMAL DESIGN IN FIG. 5.

r_1 (mm)	r_2 (mm)	r_3 (mm)	L_{pi} (mm)	r_{Li} (mm)
27.6	80.0	65.1	73.9	10.0
r_{mi} (mm)	r_{Bi} (mm)	r_{ui} (mm)	α_1(deg)	α_2(deg)
20.4	63.0	50.6	22.0	24.4

VI. CONCLUSION

In this paper we have presented new finger mechanisms in the form of modular underactuated mechanisms with features of low-cost and easy-operation. Design considerations for modular underactuated mechanisms are analyzed to identify and formulate design criteria. Design problems have been formulated in a multi-objective optimization problem that has been solved by taking into account computational characteristics of the optimality criteria. An example of optimality design has been reported as applied to an enhancement of the finger mechanisms for the LARM Hand.

REFERENCES

[1] M. C. Carrozza, C. Suppo, F. Sebastiani, B. Massa, F. Vecchi, R. Lazzarini, M. R. Cutkosky, P. Dario, "The SPRING hand: development of a self-adaptive prosthesis for restoring natural grasping", *Autonomous Robots*, vol. 16, pp. 125-141, 2004.

[2] J. Yang, E. P. Pitarch, K. Abde l-Malek, A. Patrick, L. Lindkvist, "A multi-fingered hand prosthesis", *Mechanism and Machine Theory*, vol. 39, pp. 555–581, 2004.

[3] R. Cabas, L. M. Cabas, C. Balaguer, "Optimized design of the underactuated robotic hand", in *Proc. 2006 IEEE Int. Conf. Robotics and Automation*, pp. 982-987.

[4] S. Krut, "A Force-Isotropic Underactuated Finger", in *Proc. 2005 IEEE Int. Conf. Robotics and Automation*, pp. 2314-2319.

[5] N. Dechev, W. L. Cleghorn, S. Naumann, "Multiple finger, passive adaptive grasp prosthetic hand", *Mechanism and Machine Theory*, vol. 36, pp. 1157-1173,2001.

[6] M. Yashima, H. Yamaguchi, "Control of whole finger manipulation utilizing frictionless sliding contact-theory and experiment", *Mechanism and Machine Theory*, vol. 34, pp. 1255-1269, 1999.

[7] L. Birglen, C. M. Gosselin, "Grasp-state plane analysis of two-phalanx underactuated fingers", *Mechanism and Machine Theory*, vol. 41, pp. 807-822, 2006.

[8] W. Zhang, L. Tian, Y. Ye, L. Hao, "Study on multi-finger Under-actuated Mechanism for Robotic Hand", *Chinese Journal of Machine Design and Research*, vol. 23(6), pp. 20-26, 2007.

[9] V. Bégoc, S. Krut, E. Dombre, C. Durand, F. Pierrot, "Mechanical design of a new pneumatically driven underactuated hand", in *Proc. 2007 IEEE Int. Conf. Robotics and Automation*, pp. 927-933.

[10] Liu H., Meusel P., SeitzaN., Willberga B., Hirzingera G., Jinb M.H., Liub Y.W., Weib R.. Xie Z.W. The modular multisensory DLR-HIT-Hand. Mechanism and Machine Theory 2007; 42: 612-625.

[11] M. Yong-Mo, "Bio-mimetic design of finger mechanism with contact aided compliant mechanism", *Mechanism and Machine Theory*, vol. 42, pp. 600-611, 2007.

[12] LARM homepage (2008). Available: http://webuser.unicas.it/weblarm/

[13] G. Carbone, S. Yao, M. Ceccarelli, Z. Lu, "Design and Simulation of a New Underactuated Mechanism for LARM Hand", in *Proc. 2008 Int. Conf. Theory and Practice of Robots and Manipulators*, pp. 253-260.

[14] S. Yao, M. Ceccarelli, G. Carbone, Z. Lu. "An Optimal Design for a New Underactuated Finger Mechanism", in *Proc. 2nd European Conf. Mechanism Science*, Cassino, 2008, pp.149-157.

[15] C. M. Gosselin, "Adaptive robotic mechanical systems: A design paradigm", *ASME Journal of Mechanical Design*, vol. 128(1), pp. 192 – 198. 2006;

[16] J. Gao, K. W. Chase, S. P. Magleby, "Comparison of assembly tolerance analysis by the direct linearization and modified Monte Carlo simulation methods", in *Proc. 1995 ASME Int. Design Engineering Technical Conf.*, pp. 353-360.

[17] J. W. Wittwer, W. K. Chase, L. L. Howell, "The direct linearization method applied to position error in kinematic linkages", *Mechanism and Machine Theory*, vol, 39, pp. 681-639, 2004.

[18] *The student edition of MATLAB: version 5, user's guide*, New Jersey: Prentice-Hall, Inc. D. Hanselman, B. Littlefield, 1997.